Spanish Journal of Agricultural Research (2004) 2(4), 576-587

Fertigation guidelines for furrow irrigation

G. N. Sabillón[1] and G. P. Merkley[2]*

[1] *Development Alternatives, Inc. 7250 Woodmont Av. Bethesda. MA 20814. USA*
[2] *Biological and Irrigation Engineering Dept. Utah State Univ. Logan. UT 84321. USA*

Abstract

A mathematical model was developed to simulate the application efficiency and uniformity of water-soluble fertilizers through furrow irrigation. The model simulates solute mass balance and transport for one-dimensional unsteady flow during the advance and post-advance phases of a furrow irrigation event. The model was programmed to determine the best timing and duration of fertilizer injection using two performance indices: solute application efficiency and solute application uniformity. The results from the model were compared with two sets of field data and were found to be in close agreement in terms of advance trajectories and surface water solute concentrations. Nearly 50,000 simulations were performed with the model and the results were analyzed in terms of best injection start and end times for fertilizer application efficiency and uniformity. It was found that the best injection duration time was from 5 to 15% of the time of cutoff for a complete irrigation. Most of the cases showed that the injection should take place in a relatively short time span, and at a relatively high injection rate.

Key words: hydraulic model, chemigation.

Resumen

Guías de fertirriego para riego por surcos

Se desarrolló un modelo matemático para simular la eficiencia de aplicación y uniformidad de fertilizantes solubles a través del riego por surcos. El modelo simula el balance de masa y transporte de solutos en flujo transitorio de una dimensión durante las fases de avance y humedecimiento del riego por surcos, y fue diseñado para determinar la mejor programación de la inyección de fertilizantes a través de dos índices: eficiencia de aplicación y uniformidad de soluto. Los resultados del modelo fueron comparados con dos conjuntos de datos de campo y coincidieron estrechamente en términos de trayectoria de avance de agua y concentración superficial del soluto. Con el modelo se realizaron casi 50.000 simulaciones. Se determinó que la mejor duración de la inyección fue del 5 a 15% del tiempo de corte de agua para un riego completo. En la mayoría de los casos se manifestó que la inyección debe ser realizada en un período relativamente corto y a una tasa relativamente alta.

Palabras clave: modelo hidráulico, fertirriego.

Introduction

Chemigation is the application of water-soluble chemicals (e.g. fertilizers, herbicides) through agricultural irrigation systems, including sprinkle, trickle and surface water application methods. Fertigation is the application of water-soluble fertilizers through an irrigation system, and is a specific kind of chemigation. Fertigation, as a field practice, was introduced on a wide scale in the late 1950s, and since then the technique has evolved into an advanced and a highly sophisticated technology for application of a variety of chemicals used in irrigated agriculture throughout the world. This practice is especially predominant in trickle irrigation systems, but is also commonly used in sprinkler irrigation systems. However, most of the irrigated area around the world uses surface irrigation methods, for which fertigation is not as commonly practiced. Fertigation through surface irrigation means that fertilizer is delivered by the surface water. The system should be such that the application and distribution is efficient and uniform, with minimal surface runoff at the lower end of the field, and minimal deep percolation below the crop root zone.

Perhaps the first published study on chemical application through an irrigation system was by Bryant

* Corresponding author: merkley@cc.usu.edu
Received: 03-02-04; Accepted: 29-07-04.

and Thomas (1958). Threadgill, cited by Eisenhauer (1994), estimated that approximately 11 million acres of land were chemigated in the United States in 1983. Threadgill also estimated that only 3.5% of the surface-irrigated area was under chemigation, despite numerous benefits (Dowler, 1993; Eisenhauer, 1994, after Threadgill, 1991; Chandler, 1994, after Threadgill, 1991).

Fertigation in general, when well-managed, can provide relatively uniform and timely applications of agricultural chemicals based on soil physical and chemical characteristics, and crop requirements. It can reduce soil compaction by limiting the need for tractors in the field. It reduces operator exposure to direct contact with agricultural chemicals, eliminates mechanical crop damage caused by ground sprayers, saves energy, and reduces environmental hazards. On the other hand, reduced yields or even crop failure may result from poor fertilizer distribution, with the consequent loss of income to farmers, and potential contamination of water supplies.

In spite of the above advantages, there has been relatively little use of fertigation in surface irrigation. The inherent management problems associated with this irrigation method, particularly with furrows, may be a primary cause. Uniformity, runoff, and deep percolation are the major factors to be controlled in furrow fertigation, whereas poor fertilizer management will often result from low irrigation uniformity. The majority of furrow irrigation systems are operated with high runoff losses, and deep percolation can occur even with high irrigation uniformity (Playán and Faci, 1997).

In pressurized irrigation systems, such as sprinkle and trickle, fertigation can be fairly simple, and guidelines are available for the timing of fertilizer injections during irrigation events. However, with surface irrigation, the practice of fertigation becomes much more complex because the water is distributed over the field surface, and soil infiltration characteristics are space- and time-dependent. With surface irrigation, the «best» timing of fertilizer injections into the water at the head (upstream) end of a field is not easily determined. Slight changes in the injection start and end times can dramatically affect the efficiency and uniformity of fertilizer application.

The training of farm labor in operational and management procedures such as the timing of application, concentrations and types of chemicals, coupled with appropriate safety regulations, are needed in order to make fertigation through surface methods a widespread tool in modern irrigated agriculture. Computer modeling presents an effective tool to maximize water and fertilizer application efficiencies, and distribution uniformity of any irrigation system (Abbasi *et al*., 2003). In the present research work, a surface irrigation model was developed to simulate the unsteady hydraulics of furrow irrigation and to describe the movement of a water-soluble chemical with the irrigation water. The model accounts not only for the hydraulics of water application and distribution, but also describes the transport of the solute over the soil surface, its infiltration into the soil, and along the field length, after the chemical is injected at the upstream end of the field.

Mathematical model

Although models exist for the simulation of surface irrigation hydraulics, an existing model was modified extensively to suit the particular needs of this research, and to include an equation for solute mass balance. The hydraulic simulation model for solute transport in furrow irrigation consists of three governing equations and an implicit numerical solution approach. Two of the equations are those of Saint Venant (Henderson, 1966), and the third equation is for solute mass balance. These are expressed as:

Continuity:

$$\frac{\partial Q}{\partial x}+\frac{\partial A}{\partial t}+\frac{\partial Z}{\partial t}=0 \qquad [1]$$

Motion:

$$\frac{1}{g}\frac{\partial Q}{\partial t}+\frac{\partial}{\partial x}\left(P+\frac{Q^2}{gA}\right)-AS_O+D-\frac{QI}{gA}=0 \qquad [2]$$

Solute mass balance:

$$\frac{\partial M}{\partial t}+\frac{Q}{A}\frac{\partial M}{\partial x}=0 \qquad [3]$$

where Q is discharge ($m^3 s^{-1}$); A is cross-sectional area of flow (m^2); I is infiltration rate ($m^2 s^{-1}$); g is the ratio of weight to mass (9.81 m s^{-2}); Z is cumulative infiltrated subsurface area (m^2), or volume per unit length of furrow; S_o is longitudinal bed slope (m m^{-1}); S_f is the energy loss gradient (m m^{-1}); M is the concentration of the solute chemical or fertilizer (kg m^{-3}); x is distance in the direction of flow (m); and t is time (s). The right side of Eq. 3 is taken to be zero, meaning that molecular dispersion of the fertilizer in the water has a negligible effect. This is usually the case in surface irrigation because turbulent mixing essentially negates the effects of diffusion.

A solute transport model described by García-Navarro *et al.* (2000) uses the following more general form of Eq. 3:

$$\frac{\partial(hM)}{\partial t}+\frac{\partial(huM)}{\partial x}=\frac{\partial}{\partial x}\left(hK_x\frac{\partial M}{\partial x}\right) \quad [4]$$

where h is depth of water (m); u is depth-averaged velocity (m s^{-1}); and K_x is a longitudinal dispersion coefficient (m^2 s^{-1}). Equation 4 was applied in this model using the splitting technique described by Karpik and Crockett (1997), with K_x equal to 0.075 m^2 s^{-1}, as given by García-Navarro *et al.* (2000), but the simulation results were not significantly affected for the range of cases included herein. Therefore, Eq. 3 was used instead of Eq. 4 in a simultaneous solution, together with the equations of continuity and motion.

The *pressure* term, P, is defined as:

$$P=\int_0^y A\,dy=h_cA \quad [5]$$

where y is a variable of integration (m); h_c is the depth from the water surface to the centroid of the flow area (m); and P is in m^3. The *drag* term, D, is the product of area and energy loss gradient, which is defined by the Chezy equation as:

$$D=AS_f=W_p\left(\frac{Q}{C_zA}\right)^2 \quad [6]$$

where C_z is the Chezy coefficient, a function of furrow size, surface roughness, and Reynolds number; and W_p is the wetted perimeter in the furrow (m).

The infiltration rate, I, can be defined as dZ/dt, where Z is a function of intake opportunity time, τ, from the Kostiakov-Lewis equation (Walker, 1989) as:

$$Z=k\tau^a+f_0\tau \quad [7]$$

where a and k are empirically-fitted parameters, depending on soil texture and structure, water content, and other factors; f_0 is the basic infiltration rate (m^2 s^{-1}); τ is intake opportunity time (s); and Z is in m^2. In this study, τ was defined as the time of cutoff minus the time of advance to a given distance along the furrow.

Integrated forms of the equations

The integrated forms of the three governing equations are based on interpolations within a computational cell in time and distance along the furrow, bounded by the spatial and temporal steps within the domain of the solution. Each computational cell is bounded by nodes in the x-t plane, and the solution yields dependent variable values at each node, whereby the integrated forms of the governing equations are written cell-by-cell, such that the number of equations exactly matches the number of unknown dependent variables. The dependent variables are Q, A, and M. All unknowns are located at the t + Dt timeline (Fig. 1). The four nodes defining each rectangular cell are labeled L, R, J, and K for brevity in the equations given below, instead of lengthier subscripts such as «t + Dt, x + Dx.»

The solution approach is implicit because it simultaneously solves for all unknown values at 40 to 50 computational nodes in the spatial domain at each time step, requiring the solution of several dozen equations. Initial guesses are determined at each time step for each of the unknowns, and the Newton-Raphson procedure is used to iteratively solve for the unknown values, within specified tolerance criteria. The integrated forms of the governing equations are given in Eqs. 8-12.

Continuity equation:

$$\int_t^{t+\Delta t}\int_x^{x+\Delta x}\frac{\partial Q}{\partial x}\,dx\,dt+\int_x^{x+\Delta x}\int_t^{t+\Delta t}\frac{\partial A}{\partial t}\,dt\,dx+\int_x^{x+\Delta x}\int_t^{t+\Delta t}\frac{\partial Z}{\partial t}\,dt\,dx=0 \quad [8]$$

Following the relative node nomenclature introduced in Fig. 1:

$$F_I=\left[\theta(Q_R-Q_L)+(1-\theta)(Q_K-Q_J)\right]\Delta t+\left[\phi(A_L-A_J+Z_L-Z_J)+(1-\phi)(A_R-A_K+Z_R-Z_K)\right]\Delta x=0 \quad [9]$$

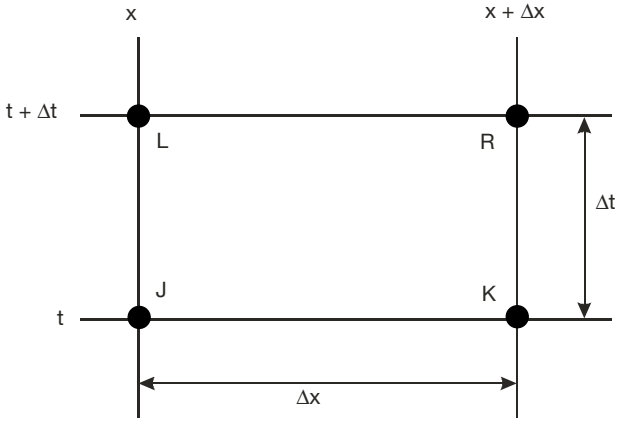

Figure 1. Computational cell nomenclature in the x-t plane.

Equation of motion (integrated as in Eq. 9):

$$F_{II} = \frac{\left[(1-\phi)(Q_R - Q_K) + \phi(Q_L - Q_J)\right]}{g\Delta t} + \quad [10]$$

$$+\frac{\theta}{\Delta x}\left[\frac{Q_R^2}{g A_R} + P_R - \frac{Q_L^2}{g A_L} - P_L\right] + \frac{(1-\theta)}{\Delta x}\left[\frac{Q_K^2}{g A_K} + P_K - \frac{Q_J^2}{g A_J} - P_J\right] -$$

$$-S_0\left\{\phi\left[\theta A_L + (1-\theta) A_J\right] + (1-\phi)\left[\theta A_R + (1-\theta) A_K\right]\right\} +$$

$$+\left\{\phi\left[\theta D_L + (1-\theta) D_J\right] + (1-\phi)\left[\theta D_R + (1-\theta) D_K\right]\right\} -$$

$$-\theta\left[\phi\left(\frac{QI}{gA}\right)_L + (1-\phi)\left(\frac{QI}{gA}\right)_R\right] -$$

$$-(1-\theta)\left[\phi\left(\frac{QI}{gA}\right)_J + (1-\phi)\left(\frac{QI}{gA}\right)_K\right] = 0$$

Equation of solute balance:

$$\int_x^{x+\Delta x}\int_t^{t+\Delta t}\frac{\partial M}{\partial t}\,dt\,dx + \int_t^{t+\Delta t}\int_x^{x+\Delta x}\left(\frac{Q}{A}\frac{\partial M}{\partial x}\right)dx\,dt = 0 \quad [11]$$

$$F_{III} = \left[\phi(M_L - M_J) + (1-\phi)(M_R - M_K)\right]\Delta x +$$

$$+\theta(M_R - M_L)\left(\phi\frac{Q_L}{A_L} + (1-\phi)\frac{Q_R}{A_R}\right)\Delta t + \quad [12]$$

$$+(1-\theta)(M_K - M_J)\left(\phi\frac{Q_J}{A_J} + (1-\phi)\frac{Q_K}{A_K}\right)\Delta t = 0$$

where F_I is the integrated equation of continuity; F_{II} is the integrated equation of motion; and F_{III} is the integrated equation of solute mass balance. All three equations are set equal to zero, and the subscripts L, R, J, and K refer to the relative node positions (Fig. 1) around any given computational cell. All values at nodes J and K are known from the previous (or initial) time step, and all values at nodes L and R are unknown until the solution converges at each time step. Z_L and Z_R are not unknowns; rather, they are determined directly from the Kostiakov-Lewis equation based on intake opportunity time, τ. The value of θ is for temporal weighting, and the value of ϕ is for spatial weighting, where $0.5 \le \theta \le 1.0$, and $0.5 \le \phi \le 1.0$. The values of θ and ϕ were both set at 0.6 in all simulations.

Field experiments

Field experiments were conducted on two furrows, each with different solute injection parameters, to compare with the simulation results from the mathematical model. The field trials took place at the Utah State University (USU) Greenville Farm in North Logan, Utah. The average longitudinal ground slope in the direction of flow was 0.0111 m m^{-1}, and was highly uniform. The scope of the field work included the following:

— The solute injection took place in a single continuous pulse and at a constant rate during the irrigation for each of the furrows, and approximately the same solute concentration was used in each furrow;

— Water samples were taken from the source of the irrigation water and the solute at the beginning and end of the injection period, and also on each of the furrows at four different locations, on a ten-minute interval, after solute injection was started;

— The locations for the water samples were: 0, 60, 120, and 180 m;

— Measurements of water advance time were taken every 10 m along the furrows;

— Measurements of furrow inflow and outflow rate were taken at preset intervals; and,

— Furrow cross-sectional profile data were obtained after each irrigation. It was found that the post-irrigation furrow cross-sections could be adequately approximated by a trapezoid.

Injection pumps, solute concentration and injection procedures

Pumps were used for the injection of the potassium bromide (KBr) tracer during the field experiments (Fig. 2). The average concentration of applied potassium bromide was 422.5 kg m^{-3} for the two furrows, both of which had free-draining outlets at the downstream end of the field. The pumps were located at the upstream

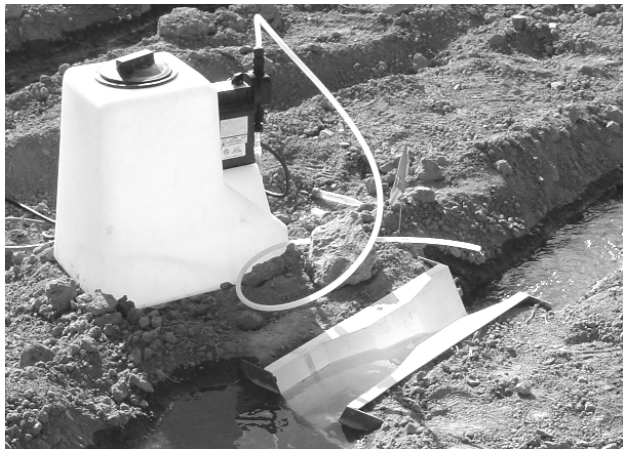

Figure 2. Solute injection at the upstream end of Furrow 1.

end of the respective furrows, with the dispensing outlet at the downstream side of a trapezoidal measuring flume. Two furrows, with buffer furrows in between, were selected for observation and the tracer solution was injected into the furrow stream at three different application times in order to determine the chemical application timing effect during each of the irrigation events. The advance phase was the reference in each furrow for the start and end of the solute injection. Following is a description of the injection procedure.

In Furrow 1, solute injection was initiated when the irrigation started, and ended when the advance phase was completed. The irrigation event continued until the solute concentration was below the detection limit at the end of the furrow. In Furrow 2, injection started when the advancing front reached half of the furrow length during the advance phase, and continued for 20 min after the end of the advance phase. Irrigation continued until no significant concentration of solute was detected at the end of the furrow.

The irrigation water was supplied through a trapezoidal concrete-lined canal. Siphon tubes with a 3.2 cm inside diameter were used to transfer water from the concrete-lined canal to the furrows of the test plot. The inflow rate was monitored whereby the water was initially discharged through the buffer furrows without any solute injection. After the inflow rate reached a desired value, the flow was diverted into the test furrows. Table 1 shows a summary of the irrigation events. Two irrigation events were necessary for testing the chosen injection timings. Furrows 1 and 2 were injected during the first irrigation, which lasted 216 min for Furrow 1, and 214 min for Furrow 2. The second irrigation event took place two days later and lasted 94 min.

The furrows were staked every 10 m for a total of 20 flagged stations (0-190 m). Advance data were recorded simultaneously in Furrows 1 and 2 during the first irrigation-injection event. Outflow data were taken following the completion of the advance phase, and until cutoff time. A trapezoidal flume and a bucket were used at the upstream and downstream ends of each furrow for measuring inflow and outflow. The cutoff time was equal to the time when furrow outflow was confirmed to be stable, thereby allowing a determination of the basic intake rate, f_o, from the inflow-outflow hydrographs.

Table 1. Irrigation data summary for the field test

Parameter	Furrow 1	Furrow 2
Q_{in} (m^3 s^{-1})	0.000918	0.000893
Q_{out} (m^3 s^{-1})	0.000445	0.000452
Advance phase (min)	61	59
Solute injection (min):		
— Start time	0.0	21.5
— End time	61.0	79.4
Time of cutoff (min)	216.0	214.4
Furrow length (m)	190.0	190.0
Furrow slope (m m^{-1})	0.0111	0.0112

Water samples were collected in the furrows at each designated sampling station: in Furrow 1 when the advancing front reached each sampling station; in Furrow 2, water sampling started in all stations when injection began (advance phase half completed). The samples were taken 10 min apart at each station immediately after injection started in each of the two furrows. After injection had ended, flow sampling was terminated as soon as the electrical conductivity (EC) of the runoff water was within three significant digits to that of the source water.

An Orion® combination bromide electrode, model 96-35 *ionplus*® (an Ion Selective Electrode), was used in conjunction with a Direct Concentration Readout Specific Ion Meter (model 720A) to determine the bromide concentration of the field samples. Bromide concentration readings (g L^{-1}) were taken by submerging the electrode in 10 ml of the sample after adding 0.2 ml of an ionic strength adjustor and a solution of 5 M $NaNO_3$ to adjust the sample to a constant background ionic strength.

Field experimental results

The field-calibrated Kostiakov-Lewis infiltration function parameters (a, k, and f_o) were determined by volume balance calculations based on the measured water advance and outflow hydrograph data (Table 2). The results of the water sample analysis from the four stations in each furrow are shown in Figs. 3 and 4. In the graphs, each of the curves represent one station sampled according to the timing set by the injection procedure, as explained above. Sampling in Furrow 1 was initiated when the advancing waterfront reached the respective station, and every 10 min after that; consequently, the sampling time is not uniform between stations (particularly for Furrow 1). Station 1 (0 m) had the greatest variability in this particular furrow.

Table 3 summarizes the results of the laboratory analysis. The most important values to compare in this table are the «Field-injected KBr» (kg) which is the

Table 2. Kostiakov-Lewis infiltration parameters for the two furrows

	Furrow 1	Furrow 2
Parameter		
Slope, S_o (m m^{-1})	0.0111	0.0112
Inflow, Q_{in} (m^3 s^{-1})	0.000918	0.000895
Kostiakov parameters		
a	0.21	0.18
k	0.0046	0.0048
f_o (m^2 s^{-1})	0.0000025	0.00000238

amount of potassium bromide injected at the upstream end of each furrow, and the «Average KBr applied» (kg) computed from the volume of water applied during the injection period and the overall average KBr concentration obtained from all stations and times. The differences were 0.20 kg and 0.12 kg, corresponding to Furrows 1 and 2, respectively. These values represent differences of 9.3% and 5.9%, respectively. The results of the laboratory analysis on the water samples were found to be acceptable, taking into account that the differences in concentration between the results of the laboratory analysis and the average computed from the field data are not significant, according to the degree of accuracy obtainable from the laboratory equipment.

In Table 3, the field-injected KBr equals solute volume injected multiplied by sampled injection tank KBr concentrations, and the volume of water applied during injection equals the integration of the hydrograph for Q_{in} over the injection interval. Water EC measurements were taken at the downstream end of each furrow.

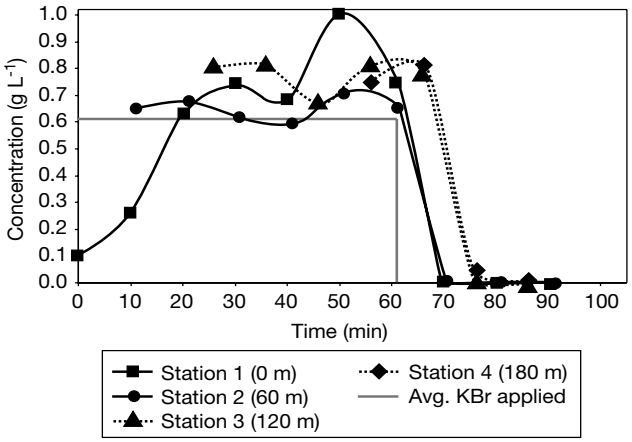

Figure 3. Solute concentration in Furrow 1 at each sampling station.

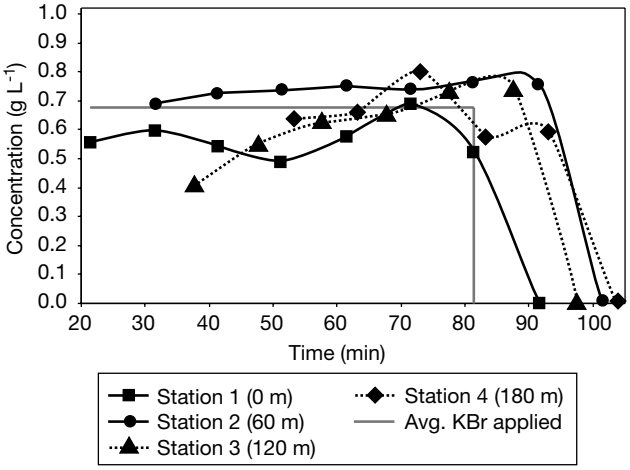

Figure 4. Solute concentration in Furrow 2 at each sampling station.

Model and field data comparisons

Field data were used to validate the mathematical model. For Furrow 1, the calibrated Kostiakov parameters were: a = 0.21; k = 0.0046; and f_o = 0.00015. The injection tank had 0.005 m^3 of solute (KBr), and an injection rate of 0.0000014 m^3 s^{-1} during the first 61 min of the irrigation event. The concentration of KBr in the tank was 413 kg m^{-3}. The source water inflow rate was measured at 0.00092 m^3 s^{-1}, so the combined furrow inflow rate was 0.00092 + 0.0000014 m^3 s^{-1} ≈ 0.00092 m^3 s^{-1}. Figure 5 shows the measured and calculated advance trajectories for Furrow 1, including results from

Table 3. Summary of the laboratory analysis on the water samples and KBr mass balance

Parameter	Furrow 1	Furrow 2
Injection time:		
— Started (min)	0.0	21.5
— Ended (min)	61.0	79.4
— Lapsed time (min)	61.0	57.9
Solute tank volume (m^3):		
Amount injected	0.0050	0.0050
Injection rate (m^3 s^{-1})	0.00000137	0.00000143
Average KBr applied (kg m^{-3})	0.614	0.676
Sampled injection tank KBr concentration (kg m^{-3})	413	420
Field-injected KBr (kg)	2.06	2.10
Water EC (dS m^{-1}):		
— Before injection	0.57	0.57
— During injection	1.22	1.22
— After injection	0.59	0.58

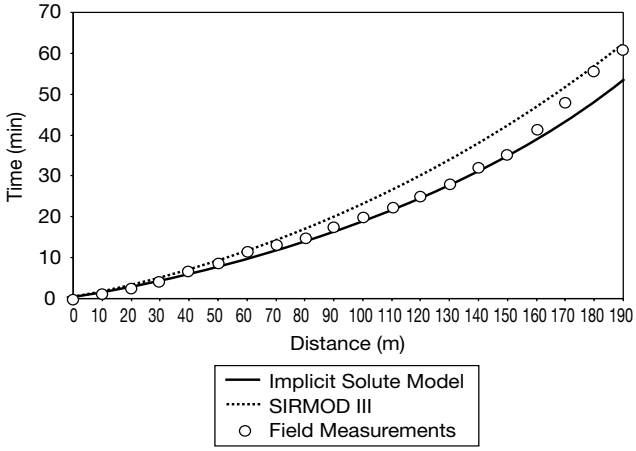

Figure 5. Comparison of measured and simulated advance trajectories for Furrow 1.

the hydrodynamic model in *SIRMOD III* (Walker, 2002), and the model described herein. Both models adequately approximated the measured advance trajectory.

Figure 6 shows the measured and simulated solute concentrations in the surface water (in the furrows) for Furrow 1 through the time at which all measurable traces of the solute were washed out of the furrow. During the initial 60 min of simulation time, the simulated solute concentration was equal to the measured concentration (within two significant digits), at a constant value of 0.61 kg m^{-3}. It is seen that the comparison between field measurements and the model is very good. After about 90 min of simulation time, the calculated solute concentrations in the surface water stabilized at zero, which was expected because the source water had a zero (or at least smaller than that which could be measured) concentration of the solute chemical. However, it is also

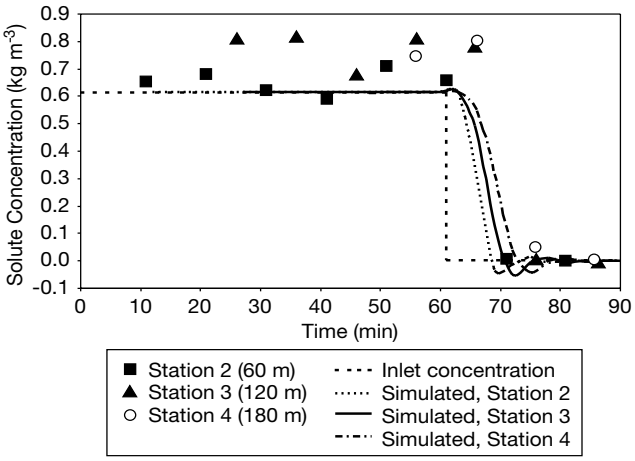

Figure 6. Comparison of measured and simulated concentrations at stations 2, 3 and 4 for Furrow 1.

seen that the model-generated results show fluctuations between 68 and 85 min of elapsed time in which the calculated solute concentrations were slightly below zero until they stabilized at zero after 85 min. Negative solute concentrations are, of course, not reasonable and are not expected to occur in practice, but in the simulations the fluctuations were always of small relative magnitude and ephemeral.

Timing of solute injection

The best timing of solute injection, meaning start (t_{start}) and end (t_{end}) times for the application of a specified volume of concentrated solute, was determined from multiple simulations using the hydraulic model, not through the application of a mathematical optimization algorithm. Although optimization could have been used, the runs were fast enough that the more computational exhaustive approach was chosen. This approach also eliminated the possibility of an optimization algorithm stopping at a local maximum of the objective function.

The difference in start and end times determined the required constant rate of injection for the specified volume of solute in a chemical tank at the head end of the furrow. Each simulation was for a uniform, sloping furrow and free-draining outlet conditions (at the downstream boundary). All simulations were for a «complete irrigation» that is, the least-watered location along the entire field length, from 0 to L, received a subsurface infiltrated area (volume per unit length) equal to the specified root zone water deficit, Z_{reqd} (m^2). This means that the time of cutoff was set equal to the time of advance to the end of the furrow, t_L, plus the required intake opportunity time, τ_{reqd}, which was calculated by iteration from the specified Z_{reqd} and Kostiakov-Lewis equation (Eq. 7) parameters. The time of recession was assumed to be negligible and was not taken into account for determining intake opportunity times. This assumption is valid for most sloping and free-draining furrows, especially when the irrigation is complete.

Calculation of solute storage

A vertically-inverted variation of the cumulative infiltration profiles must be used to account for the layering effect from the ground surface downward, thereby taking into account the vertical movement of solute. Figure 7 shows how the soil water solute concentrations move downward from the ground

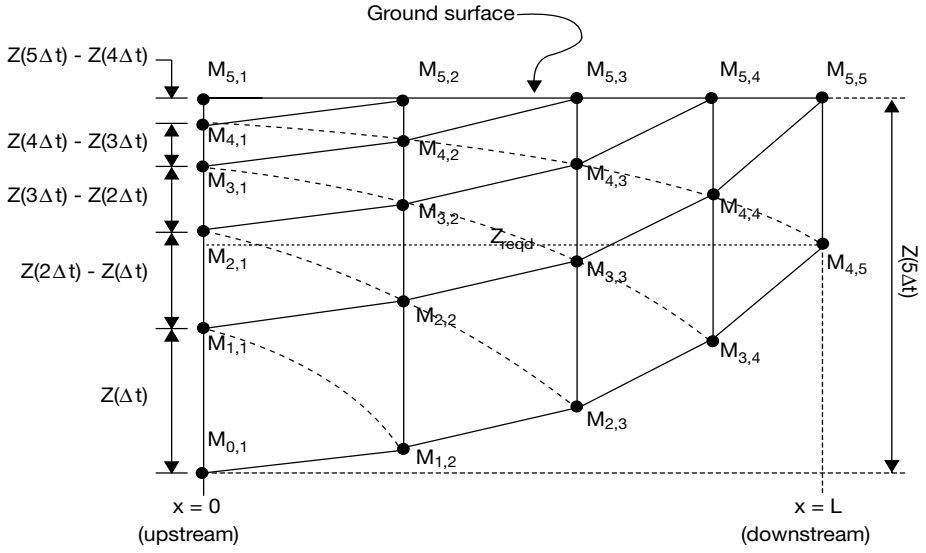

Figure 7. Sample subsurface soil water solute concentration profiles at time of cutoff for a complete irrigation after five time steps.

surface in successive layers, which must be accounted for in the simulation model so that the amount of solute lost below the root zone, in the form of deep percolation, can be quantified. The trapezoidal subsurface cells of constant solute concentration distort as they move vertically downward with each time step, whereby the sidewalls remain vertical and the other two walls move asymptotically toward the horizontal, according to the functional form of the Kostiakov-Lewis equation.

At the end of a complete irrigation, in which the entire field length receives a specified infiltration of at least Z_{reqd}, the cumulative infiltrated depth of water at the downstream end of the furrow ($x = L$) will be approximately equal to Z_{reqd}. Figure 7 shows sample infiltration profiles for a complete irrigation that finishes after five time steps, where the curves of equal time step are dotted, and the time step is denoted by the first subscript on the M (solute concentration) terms. The second subscript on the M terms represents the physical location along the field length. Then, knowing the Z values corresponding to each subsurface node, the total mass of solute contained in the root zone (between the ground surface and Z_{reqd}) at the time of cutoff can be determined.

The first step in the computation of the solute mass in the root zone is to determine the interpolated M values at the Z_{reqd} depth, using the known values straddling the Z_{reqd} line, above and below. Next, the M values above the Z_{reqd} line are averaged at each discrete distance along the field, and the total mass is summed. Solute mass lost as surface runoff was tabulated in the computer program according to the runoff flow rate and the solute concentration at $x = L$ for each time step after the time of advance. The initial solute mass leaving the furrow as runoff, at the end of the advance phase, is calculated based on interpolations. Similarly, the solute mass entering the furrow at $x = 0$ was computed during the irrigation event. With these and the calculated root zone solute mass, the solute mass lost due to deep percolation (infiltrated beyond the root zone boundary) is calculated by mass balance, with the simplifying assumption that the solute moves freely with the water through the soil profile.

In the computer program, the M values for soil water are stored in a two-dimensional array with fixed dimensions and moving row indices such that a sufficient number of values are retained and the total root zone solute mass can be calculated as described above. This is premised on the fact that none of the M values that are more than one node below Z_{reqd} are needed to determine root zone solute mass. Corresponding Z values are stored in a column vector that is linked to the M array, also recognizing that there are a maximum of $t_{co}\Delta Z/\Delta t$ values in the subsurface infiltration grid, where t_{co} is the time of cutoff (s), and Δt is the fixed time step (s). This coding approach reduces both the program's memory requirements and the execution time.

Uniformity and efficiency calculations

Two performance indices were computed for each simulated irrigation event. Solute application efficiency, E_{sa}, was defined as a fraction:

$$E_{sa} = \frac{m_{rz}}{m_{in}} \quad [13]$$

where m_{rz} is the mass of solute in the root zone at the end of the irrigation (kg); and m_{in} is the mass of solute injected at the upstream end of the furrow (kg). The solute coefficient of uniformity, CU_{sa}, was computed as a weighted average because of the nonlinear node spacing that arises during the advance phase with a constant time step:

$$CU_{sa} = 1.0 - \frac{n\sum_{i=1}^{n}\left[abs\left(M_{avg,i} - \bar{M}_{avg}\right)\Delta x_i\right]}{L\sum_{i=1}^{n} M_{avg,i}} \quad [14]$$

where $0 \le CU_{sa} \le 1$; n is the number of spatial nodes; L is the furrow length (m); $M_{avg,i}$ is the time-averaged solute concentration at spatial node i; and $\bar{M}_{avg}$ is the weighted average of all the $M_{avg,i}$ values (kg m^{-3}). $\bar{M}_{avg}$ was calculated as follows:

$$\bar{M}_{avg} = \frac{1}{L}\sum_{i=1}^{n}\left(M_{avg,i}\Delta x_i\right) \quad [15]$$

It is noted that the equation for CU_{sa} is a modified form of Christiansen's uniformity coefficient (Christiansen, 1942), which was developed for sprinkle irrigation evaluations.

The «objective function» for the optimization process was to maximize the product of E_{sa} and CU_{sa} for each case by independently varying the injection start and end times. It was reasoned that the product of the two terms would adequately represent water application efficiency and uniformity of water application because neither is sufficient by itself if the other is of low magnitude. The limits on injection start time were that it was greater than or equal to zero and less than the time of advance to the end of the furrow, t_L. This required that the advance time be calculated by the model before beginning the evaluation process for each case. The injection end time had to be at least one time step beyond the injection start time, and less than or equal to the time of cutoff, t_{co}. Thus, the objective function had the following numerical range:

$$0 \le E_{sa}CU_{sa} \le 1 \quad [16]$$

where a value of «1» means perfect efficiency (all the solute stayed in the root zone) and perfect solute application uniformity.

The water application efficiency, E_a, was also calculated in the model, where E_a is the ratio of the volume of water stored in the crop root zone immediately after an irrigation to the volume of water applied at the upstream end of the furrow during the irrigation. Both surface runoff and deep percolation losses result in a lowering of the E_a value.

Solute distribution simulations

Nearly 50,000 hydraulic simulations were performed, with different combinations of field parameter values. Parameter variations included furrow inflow rate, furrow length, longitudinal furrow slope, required infiltration depth, and Kostiakov calibration values. The model was set up to search for the highest value of the objective function ($E_{sa}CU_{sa}$) for each set of parameters by varying the solute injection start and end times. The amount of injected solute was the same for each simulation, as was the solute concentration in the tank, so that the simulated injection rate varied according to the difference in start and end times; that is, the same volume of solute was injected in each simulation.

The mathematical model was configured to run batches of simulations with differing parameter values. Convergence tolerances for the solution of the equations were ± 0.000001 m^2 for cross-sectional area, and ± 0.00001 m^3 s^{-1} for flow rate. Parameter variations included field length, longitudinal field slope, inflow rate, required application depth, and Kostiakov infiltration parameters. The Kostiakov «a» exponent was varied from 0.1 to 0.5 in increments of 0.1, covering a range of exponents often found in the field. The Kostiakov «k» value was held constant at 0.001 for all simulations. The basic intake rate, f_o, was set at 0.0001 m^2 min^{-1} in all simulations. Field length was varied from 200 to 300 m, also common lengths, and the furrow longitudinal slope was varied from 0.0025 to 0.01 m m^{-1}. For each combination of parameter values, 420 different combinations of solute injection start and end times were tested in the model, and the best of these was recorded to a text file. The «best» simulation performance was evaluated as a combination of efficiency and uniformity of solute application, as described below.

Before running the 420 simulations for each parameter combination, a partial simulation was executed to determine the advance time, t_a. Then, 21 different injection start times (t_{start}) were tested in simulations, beginning with zero (the start of the irrigation), then 5% of the advance time ($0.05t_a$), 10% of the advance time ($0.10t_a$), and so on, up to t_a. Thus, the start of solute injection never exceeded the time of advance. Finally, 20 different end times (t_{end}) for solute injection were tested

for each solute start time: $t_{end} = t_{start} + 0.05\ (t_{co}-t_{start})$; $t_{end} = t_{start} + 0.10(t_{co}-t_{start})$; and so on, up to $t_{end} = t_{co}$. The combination of 21 values of t_{start} and 20 values of t_{end} gave the 420 simulations for each parameter combination.

The water application efficiency of the irrigation event, defined as the volume of water stored in the root zone divided by the total volume of water applied at the head end of the furrow, was also calculated for each simulation. However, the application efficiency, E_a, was very nearly constant for the variations in injection start and end times (all other parameters the same), so it did not impact the objective function in determining the «best» start and end times. The first set of simulations were for continuous inflow of water at the head end of the furrow, but these invariably gave low water application efficiencies, so the final set of simulations were performed for «cutback irrigation» in which the furrow inflow was reduced as soon as the water had advanced to the end of the furrow. This practice is common in many areas in the western USA and provides higher water application efficiency than continuous flow by reducing the surface runoff at the end of the furrow, but does not significantly affect the deep percolation losses because the time of cutoff remains the same for a «complete» irrigation, as defined above.

The initial flow rate into the furrow was determined as a function of the longitudinal ground slope, S_o, according to a maximum nonerosive stream size. This was taken to be $Q_{in} = 0.0007/S_o$, where Q_{in} is the furrow inflow rate during the advance phase, in $m^3\ s^{-1}$, and S_o is in percent. The coefficient 0.70 is an average value for «erodible» soils (USDA, 2002), which is appropriate for many soil types in agricultural fields. The initial (before cutback) value of Q_{in} varied from 0.0007 to 0.0028 $m^3\ s^{-1}$ for the slopes considered herein, and the cutback inflow rates were from 0.00046 to 0.00175 $m^3\ s^{-1}$. At the end of the advance phase, when water reached the downstream end of the furrow, the instantaneous infiltration rate, I, was estimated by integration along the furrow length, and the inflow was reduced to 105% of this value.

The downstream boundary was a free-draining furrow outlet, based on the Chezy equation. The Chezy «C» value was set to 50 for all simulations. The volume of solute in the chemical tank was equal to 0.005 m^3 for each simulation, with a tank concentration of 500 kg m^{-3}; the source water solute concentration was zero. The furrow cross section was approximated by a symmetrical trapezoid with a base width of 0.10 m, and an inverse side slope of 1.5.

Analysis of simulation results

Considering all simulation results (not only those with the best values of the objective function), it was observed that the mass of solute retained in the root zone was zero in the worst cases, meaning that all of the infiltrated solute was leached out of the root zone before the end of the irrigation. In such cases, the timing of solute injection was clearly inappropriate. The product of E_{sa} and CU_{sa} was best, on average, for a Kostiakov «a» of 0.3; it decreased both for «a» < 0.3 and for «a» > 0.3.

In all the simulations, the water application efficiency, E_a, varied from 33 to 80%, with an average value of 56%. However, as noted above, the E_a was not a significant factor in determining the best injection times. The best injection start time was, on average, 64% of the time of advance. In approximately half of the cases, the best injection start time was less than 80% of the advance time, but in no case was the optimal injection start time more than 95% of the advance time, indicating that within the parameter ranges considered herein, it is always best to begin injection before the water reaches the end of the furrow. In no case was the best injection start time less than 5% of the advance time, meaning that injection should start some time after beginning the irrigation, at least for the parameter ranges used herein.

The best duration of solute injection was from 5 to 15% of the time of cutoff, t_{co}. Most of the results show a best duration of 5%, while only a few give a duration of more than 10% of the time of cutoff (mostly for small furrow slope values). For Kostiakov «a» of 0.1, the best injection duration decreases with increasing slope, while for «a» > 0.2 the best duration increases with increasing slope. However, for «a» of 0.2 and 0.3, the best injection duration is not a strong function of either furrow slope or length. For the best-case simulations, CU_{sa} was from 92 to 100%, and E_{sa} was from 45 to 97%. Thus, in some cases the simulation results predict the potential for highly effective fertigation in furrow irrigation.

The average value of the objective function, $E_{sa}CU_{sa}$, for different values of the Kostiakov «a» parameter, over the same range of furrow lengths and slopes, is shown in Fig. 8. It is seen that the minimum average objective function value occurs at an interpolated Kostiakov «a» value of approximately 0.25, increasing monotonically away from this «a» value. The highest average objective function value was for the highest

«a» value used in this study, which was 0.5, corresponding to the high end of the infiltration rate.

Multiple linear regression analysis was performed for the objective function, as defined by $E_{sa}CU_{sa}$, which includes efficiency and uniformity of solute application. The objective function can be adequately approximated as a linear function of slope, S_o, and furrow length, L, for the five different Kostiakov «a» values, as shown in Table 4. The equation form is as follows:

$$E_{sa}CU_{sa} = \alpha_1 S_o + \alpha_2 L + \alpha_3 \quad [17]$$

It is noted in Table 4 that the multiple regression for Kostiakov «a» of 0.3 gave a relatively high coefficient of determination ($R^2 = 0.99$), while the correlation decreased monotonically away from this «a» value. The only approximately linear relationship found was that of the objective function in terms of S_o and L; all others were highly nonlinear.

Conclusions

A mathematical model was developed to simultaneously solve the two equations of one-dimensional unsteady open-channel flow and a simplified form of a solute mass balance equation. The model assumes that the diffusion terms in the solute mass balance equation are negligible, and this was confirmed for the cases included herein through modeling tests with the more complete equation. The model also assumes that the solute moves freely with the water within the soil profile, and that the recession phase in sloping furrows is of negligible duration.

The objective function in the evaluation routines of the mathematical model was defined as $E_{sa}CU_{sa}$, and was shown to be an approximately linear function of furrow slope and length. The multiple regression slopes and intercept vary slightly with the value of the Kostiakov «a» parameter, but the results are nevertheless quite predictable. The objective function almost invariably increases with increasing slope, within the 0.0025 to 0.0100 m m^{-1} range considered in this research. The objective function also increases with increasing furrow length, at least in the 200- to 300-m range considered herein. Thus, within limits, steeper field slopes and longer furrows tend to give a better product of solute application efficiency and uniformity.

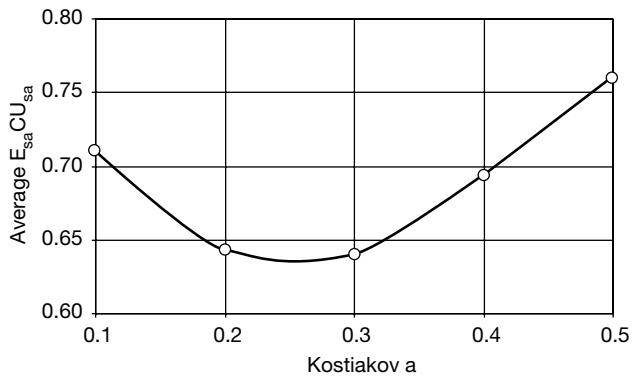

Figure 8. Average objective function value *versus* Kostiakov «a».

Table 4. Summary of multiple regression results for $E_{sa}CU_{sa}$ as a function of furrow length and slope (see Eq. 17)

Kostiakov a	α_1 (S_o)	α_2 (L)	α_3 (Intercept)	R^2
0.1	23.7	0.00091	0.333	0.90
0.2	30.2	0.00144	0.093	0.94
0.3	39.7	0.00108	0.122	0.99
0.4	43.7	0.00091	0.193	0.97
0.5	41.7	0.00086	0.285	0.94

One of the conclusions drawn from the model results was that the best injection duration time was from 5 to 15% of the elapsed time at cutoff for a complete irrigation. Most of the cases showed a value in the 5% range, meaning that the injection should take place in a relatively short time span, and at a relatively high injection rate. It is clearly disadvantageous, in all cases, to inject the solute at a low rate over a time period that is a significant fraction of the total irrigation time (time of cutoff, t_{co}). Thus, the management question is not «how long to inject the solute,» rather, «when to begin solute injection?».

The best injection start times varied from 5 to 95% of the advance time, which is a wide range of values. However, for soils with a low Kostiakov «a» value, the best injection start times were all in the 85 to 95% range, as compared to the time of advance. Consequently, when the «a» value is low, injection should begin near the end of the advance phase. For Kostiakov «a» values of 0.3 and greater, the best injection start time is much more variable. When «a» is greater than or equal to 0.3, the best ratio of injection start time to advance time always started high for low furrow slopes, decreased with increasing slope, then began increasing again at even higher slopes. For the same range of «a» values, there was no easily discernable relationship between the best injection start time and the furrow length. This behavior makes it difficult to provide general recommendations on injection start time when the soil infiltration rate is relatively high.

Acknowledgment

The authors would like to thank the support from the Utah Agricultural Experiment Station, Project 788.

Notation

a = exponent in the Kostiakov-Lewis equation;
A = cross-sectional area of flow in the furrow (m^2);
CU_{sa} = coefficient of uniformity for solute application in the crop root zone (fraction);
C_z = Chezy equation coefficient;
D = drag term in the equation of motion (m^2);
E_a = water application efficiency (fraction);
E_{sa} = solute application efficiency (fraction);
EC = electrical conductivity (dS m^{-1})
f_o = basic soil intake rate (m^2 s^{-1});
g = ratio of weight to mass (m s^{-2});
h = depth of water (m);
I = infiltration rate (m^2 s^{-1});
k = coefficient in the Kostiakov-Lewis equation;
K_x = longitudinal dispersion coefficient (m^2 s^{-1});
L = furrow length (m);
M = solute concentration (kg m^{-3});
m_{in} = total solute mass injected at the upstream end of the furrow (kg);
m_{rz} = total solute mass contained in surface runoff from the field (kg);
n = number of computational nodes along the length of the furrow;
P = pressure term in the equation of motion (m^3);
Q = flow rate (m^3 s^{-1});
Q_{in} = furrow inflow rate, at distance zero (m^3 s^{-1});
Q_{out} = furrow outflow rate, at distance L (m^3 s^{-1});
S_o = longitudinal furrow slope (m m^{-1});
t = time (s);
t_{co} = time of cutoff of the inflow to the upstream end of the furrow (s);
t_L = time of advance to the end of the furrow (s);
t_{end} = time at which solute injection ends (s);
t_{start} = time at which solute injection begins (s);
u = depth-averaged velocity (m s^{-1});
x = distance along the furrow length (m);
y = variable of integration (m);
Z = cumulative infiltrated depth of water (m^2);
Z_{reqd} = required cumulative infiltrated depth of water (m^2);
α = regression equation constant;
ϕ = spatial weighting factor;
θ = temporal weighting factor;
τ = intake opportunity time (s); and,
τ_{reqd} = required intake opportunity time (s).

References

ABBASI F., SIMUNEK J., VAN GENUCHTEN M., FEYEN J., ADAMSEN F.J., HUNSAKER D.J., STRELKOFF T.S., SHOUSE P., 2003. Overland water flow and solute transport: model development and field-data analysis. J Irrig Drain E-ASCE 129(2), 71-81.

BRYANT B.B., THOMAS E.L., 1958. Distribution of fertilizer materials applied through sprinkler irrigation systems. Bull. 598. Univ. of Arkansas Agric. Exp. St., Fayetteville, 12 pp.

CHANDLER L.D., 1994. A white paper for chemigation: development of a policy statement. XV Int. Irrig. Expos. & Tech. Conf., Fairfax, Virginia, pp. 97-102.

CHRISTIANSEN J.E., 1942. Irrigation by sprinkling. Calif. Agric. Exp. Station Bulletin 670. Univ. of California, Berkeley.

DOWLER C.C., 1993. Chemigation. In: Application technology for crop protection (Matthews G.A. and Hislog E. C., eds.). CAB International. pp. 317-327.

EISENHAUER D.E., 1994. Chemigation: another usage for your irrigation system. Irrig J 44(2), 30-31.

GARCÍA-NAVARRO P., PLAYAN E., ZAPATA N., 2000. Solute transport modeling in overland flow applied to fertigation. J Irrig Drain E-ASCE 126(1), 33-40.

HENDERSON F.M., 1966. Open channel flow. MacMillan Pub. Co., Inc. NY. 522 pp.

KARPIK S.R., CROCKETT S.R., 1997. Semi-Langrangian algorithm for two-dimensional advection-diffusion equations on curvilinear coordinate meshes. J Hydraul Eng-ASCE 123(5), 389-401.

PLAYAN E., FACI J.M., 1997. Border irrigation: field experiments and a simple model. J Irrig Sci 17(4), 163-171.

THREADGILL E.D., 1991. Advances in irrigation, fertigation, and chemigation. Fertigation/Chemigation, Proc. Expert Cons. Fert./Chem., FAO AGL/MISC 19/91. Rome, Italy.

USDA (United States Department of Agriculture), 2002. Montana, Natural Resources Conservation Service, U.S. Dept. of Agric. Available in http://www.mt.nrcs.usda.gov/pas/nutrient/nutrient.html. [10 May 2003].

WALKER W.R., 1989. Guidelines for designing and evaluating surface irrigation systems. Food and Agriculture Organization (FAO) of the United Nations, Irrig. and Drain. Paper 45, Rome, Italy. 135 pp.

WALKER W.R., 2002. SIRMOD II - Surface irrigation simulation, evaluation and design. User's guide and technical documentation. BIE Dept., Utah State Univ., Logan, Utah.